Photodynamic Therapy with Hexa(sulfo-*n*-butyl)[60]Fullerene Against Sarcoma *In Vitro* and *In Vivo*

Chi Yu[1,*], **Pinar Avci**[2,3,4], **Taizoon Canteenwala**[5], **Long Y. Chiang**[5], **Bao J. Chen**[6], and **Michael R. Hamblin**[2,3,7,*]

[1]Department of Animal Science, National Pingtung University of Science and Technology, Pingtung, 91201, Taiwan

[2]Wellman Center for Photomedicine, Massachusetts General Hospital, Boston, MA 02114, United States

[3]Department of Dermatology, Harvard Medical School, Boston, MA 02115, United States

[4]Department of Dermatology, Dermatooncology and Venerology, Semmelweis University School of Medicine, Budapest, 1085, Hungary

[5]Department of Chemistry, University of Massachusetts, Lowell, MA 01854, United States

[6]Department of Animal Science, National Taiwan University, Taipei, 10672, Taiwan

[7]Harvard-MIT Division of Health Sciences and Technology, Cambridge, MA 02139, United States

Abstract

The hydrophilic molecular micellar hexa(sulfo-*n*-butyl)[60]fullerene (FC_4S), first synthesized in 1998 as a photosensitizer (PS) has been reported to exhibit high efficacy for singlet oxygen generation and antimicrobial photodynamic inactivation. The purpose of this study was to investigate the effects of photoactivated FC_4S for free radical generation and to mediate photodynamic therapy (PDT) of cancer *in vitro* and *in vivo*. The results demonstrated that following light irradiation, FC_4S produced singlet oxygen, but after addition of electron donors such as ferrocytochrome c or NADH, FC_4S also produced superoxide. The combination of FC_4S with light irradiation was able to induce cytotoxicity to human fibrosarcoma cells and murine sarcoma 180 cells *in vitro*. Cell-killing was proportional to fluence as well as FC_4S concentration. Photoirradiation by argon-ion laser after intraperitoneal injection of FC_4S also resulted in inhibition of S180 tumor growth *in vivo* (up to 80% reduction of tumor volume). Hematological and blood biochemistry parameters of the cancer-bearing mice were improved by PDT. Based on these findings, we conclude that FC_4S has a great potential as a nanomedicine in PDT for cancer.

Keywords

Hydrophilic hexa(sulfo-*n*-butyl)[60]fullerene (FC_4S); Photodynamic Therapy; Reactive Oxygen Species; S180 Murine Sarcoma; ICR Mice

---

[*]Authors to whom correspondence should be addressed.

1. INTRODUCTION

Photodynamic therapy (PDT) is based on the combination of a non-toxic photosensitizer (PS) and light irradiation that results in eradication of malignant cells and infectious microorganisms.[1, 2] Effective PS possess the following characteristics: they have good absorption of light in the visible region, possess high efficiency of generation of singlet oxygen or other reactive oxygen species (ROS), low toxicity in dark, and are selective for the target tumor or microbial cells.[3] Fullerene (C_{60}) is a stable compound composed of 60 carbon atoms in a closed cage structure with 30 double bonds. C_{60} can give various derivatives after addition reactions across the double bonds.[4] Moreover due to the large number of double bonds (30), it is also easily excited by visible light. C_{60} has a high quantum yield of singlet oxygen in organic solvents, but switches to a photochemical mechanism involving superoxide and hydroxyl radicals in aqueous solvents.[5]

C_{60} is soluble in only a few organic solvents, therefore the bioavailability of C_{60} must be improved by enhancing water solubility with hydrophilic functional groups.[6] One concern during this process may be reduced efficacy due to fewer double bonds, however water-soluble C_{60} derivatives have been confirmed to possess good PDT activity. Following exposure of HeLa cells to two types of amino acid-C_{60} derivatives and irradiation, a marked decrease in cell viability, and an increase in malondialdehyde (MDA) production were reported.[7]

PDT using cationic C_{60} derivatives has been reported to demonstrate antimicrobial effects[8] and reduce the mortality in mice with wounds that were infected by lethal bacteria.[9] To our knowledge there have only been two previous reports concerning the use of fullerene derivatives to mediate PDT of tumors *in vivo*.[10] Tabata et al.[11] used a C_{60} derivative as a PS to inhibit tumor growth in mice. C_{60}-polyethylene glycol (PEG) was injected intravenously and C_{60}-PEG was found to remain in tumor tissue substantially longer than in muscle and skin. The dosage of 424 μg/kg of C_{60}-PEG exposed to 107 J/cm^2 of 400–505 nm light caused tumor tissue necrosis and completely inhibited tumor growth. Intraperitoneal PDT in mice with disseminated colon cancer mediated by a monocationic fullerene excited with different wavelengths of light produced good tumor response and a survival advantage.[12]

The water-soluble molecular micellar hexa(sulfo-*n*-butyl)C_{60} compound known as FC$_4$S was first prepared in 1997,[13] and a subsequent report detailed its toxicity.[14] FC$_4$S has been reported to generate singlet oxygen.[15] and exert cytotoxic effects on infectious microorganisms following light exposure.[16] The effectiveness of FC$_4$S in mediating PDT and its excellent water solubility, suggested that FC$_4$S could be a useful potential PS for mediating tumor treatment *in vivo*. Thus, FC$_4$S was used as the PS in this study to explore its effects such as ROS production and PDT cytotoxicity against murine sarcoma cells *in vitro* and its anti-tumor effects in tumor-bearing mice, *in vivo*.

2. MATERIALS AND METHODS

2.1. Preparation and Molecular Assembly Characteristics of FC_4S

The synthetic scheme and chemical structure of water-soluble molecular micellar hexa(sulfo-*n*-butyl)[60]fullerene (FC_4S), $C_{60}(CH_2CH_2CH_2CH_2SO_3Na)_6$, is shown in Figure 1(A). It was prepared by a modified direct one-pot method reported previously.[17] C_{60} in dimethoxyethane (DME) was first treated with sodium naphthalenide at 25 °C to yield hexaanionic fullerene intermediate, $C_{60}^{\square 6}$ without isolation. It was then allowed to react with an excess of 1,4-butane sultone (15.0 equiv.). After purification by filtration and repeated reprecipitation in MeOH from an aqueous solution, the FC_4S (sodium salts) product was observed and detected by a single HPLC peak using a reverse-phase C-18 column eluted with H_2O. Acidification of FC_4S with dil. HCl (4N) gave the corresponding hexasulfonic acid (FC_4SH) less soluble in H_2O that facilitates the further purification to remove water-soluble impurities. FC_4S was re-generated by treatment with NaOH in a yield of 80–85%.

The aggregation of FC_4S in water was evaluated using small angle neutron scattering (SANS) in D_2O and small angle X-ray scattering (SAXS)[18] to reveal that FC_4S formed molecular nanospheres in water, with the hydrodynamic volume being consistent with a large number of H_2O molecules trapped inside the nanosphere. This nanocluster formation results in nearly a monodisperse ellipsoid-like spheroidal shape with a radius of gyration of ~19 Å and an estimated long sphere diameter of ~60 Å, corresponding to the octahedral packing of 6 FC_4S molecules located at each vertex. The observation is consistent with hydrophobic interactions between C_{60} core cages overcoming loose charge repulsion at the molecular surface of the micelle-like FC_4S structure.

2.2. Detection of Reactive Oxygen Species in Solution and Electron Donor System

2.2.1. Measurement of Singlet Oxygen Production in Photoirradiated FC_4S Solution—Direct measurement of singlet oxygen was carried out by the detection of its luminescence at 1270 nm which corresponds to the $^1\Delta_g$ to $^3\Sigma_g$ transition of molecular oxygen.[19] A 10 μM FC_4S in various solvents (DMF, DMSO, H_2O and PBS) was placed in a quartz cuvette and then irradiated with a tunable pulse laser system (OPO Rainbow 355, OPOTEK Inc., Carlsbad, CA.) at the excitation wavelength; 512 nm or 600 nm for 2400 pulses. The photon counts were measured by a highly sensitive photon multiplier tube (PMT) detector (Model R5509-42, Hamamatsu Corp., Bridgewater, NJ) which was coupled with 4 bandpass filters (1200, 1270, 1300, and 1330 nm) and monitored in the near infrared region. The PMT output was amplified and converted to a voltage pulse using a high-speed current preamplifier (Stanford Research Systems, Model SR445). A multichannel scaler (Stanford, Model SR430) connected to a personal computer was used for time-resolved single photon counting.

2.2.2. Detection of Superoxide Radical Anion—One mL of 100 μM cytochrome c in PBS and 1.0 mL of FC_4S solution with graded concentrations (0–100 μM) were added to a 24 well plate. The mixed solution was exposed to a broad-band (400–700 nm) fluorescent light source emitting an irradiance of 8.0 mW/cm^2 for a period of 0–90 min (at a distance of 5–6 cm from the cover). The extent of cytochrome *c* reduction was evaluated by measuring

the change in absorbance at 550 nm (Beckman DU65 spectrometer). A similar experiment was carried out in the presence of superoxide dismutase (SOD) (75 or 150 units) to investigate the effect of SOD addition on the cytochrome c reduction by FC_4S.

2.2.3. FC_4S-Electron Donor System—To investigate whether the photo-production of singlet oxygen by FC_4S is affected by an electron donor, NADH was used as a reducing agent and the electron source in solution. The electron transfer process was tested using a cuvette and a crystal pulsed laser at 532 nm for irradiation. The FC_4S solution (0.4 mL, 100 μM in H_2O) was mixed with increased concentrations of NADH solutions in D_2O–H_2O (3:1), with molar ratios of NADH/FC_4S from 0–1000 times. After mixing the FC_4S/NADH solution by pipette, the mixture was irradiated by 30000 laser pulses and the photoemission was detected at infrared range as described previously.

2.3. The Cytotoxicity of Photoirradiated FC_4S on Tumor Cells *In Vitro*

2.3.1. Cell Viability—In order to test cytotoxic potential of FC_4S-mediated PDT on cancer cells, two different cell lines HT-1080 (human fibrosarcoma cells, CCRC 60037 purchased from Food Industry Research and Development Institute, Taiwan) and S180 cells (murine sarcoma 180 cells, obtained from Biochemistry and Biotechnology Institute of Chung Shan Medical University, Taiwan) were used. Cell lines were cultured in α-MEM medium with L-glutamine and supplemented with 10% FBS and antibiotics (100 units/mL of penicillin G and 100 μg/mL streptomycin sulfate). Cells were incubated in the dark in 95% humidified air plus 5% CO_2. After harvested by trypsin–EDTA, cells were resuspended in 500 μL α-MEM medium, and each suspension included 1.0×10^4 cells (fibrosarcoma and sarcoma 180 cells). Cell suspension (500 μL) of HT-1080 and S180 cells were plated into a 24-well plate and pre-incubated at 37 °C for 24 h. To each well was then added 500 μL FC_4S solution in graded concentrations (0–20 μM). After 24 h, cells were illuminated with a fluorescent light source at 8.0 mW/cm^2 for different periods of time, ranging from 0–60 min. After further incubation of the irradiated cells for a period of 48 h, a MTT method[20] was used for detection cell viability.

2.3.2. Cell Morphology—Changes in cell morphology following PDT were also investigated. The cells were maintained under the same conditions as described above. Cell suspensions (4 mL) were placed on glass coverslips and incubated with 5 μM FC_4S in a 6 well plate. 48 h following PDT, cells were fixed with freshly prepared 2.5% glutaraldehyde in PBS for 2 h at 4 °C. HT-1080 cells were stained with Giemsa solution and S180 cells were stained by Feulgen method.[21]

2.4. Inhibitory Effect of Photoirradiated FC_4S on Tumor Growth *In Vivo*

2.4.1. Animal Treatment—*In vivo* experiments were conducted in 6 weeks old, 37 ± 0.8 g, pathogen free male ICR mice [Charles River Japan origin Crl: CD-1® (ICR)BR]. Animals were housed in polycarbonate cages on hardwood bedding (5 mice/cage) under controlled conditions (temperature 22 ± 1 °C, relative humidity 55 ± 15%, and light/dark cycle 12/12 h). The mice were allowed free access to a laboratory rodent diet (# 5K55, Purina Mills, Inc., St. Louis, MO) and water available *ad libitum*.

2.4.2. Tumor Induction—The subcutaneous tumor was induced by injection of 100 μL of the S180 cell suspension (total 1×10^7 cells) in the skin region overlying the abdomen of healthy mice. The mice were selected for study when the tumor reached a diameter of 8 ± 1 mm, which took on average 5–7 days. Mice were sacrificed 30 days after tumor implantation or earlier if any dimension exceeded 2 cm diameter.

2.4.3. Experimental Groups—Sixty tumor-bearing mice were divided into 6 treatment groups (10 mice in each group), while another 10 tumor free mice were used as the control group. The treatment groups were:

1. control (no tumor implantation),

2. tumor control (only tumor implantation),

3. light control (100 J/cm^2 laser irradiation)

4. dark control (intraperitoneal injection (i.p.) of FC$_4$S (15 mg/kg) to tumor-bearing mice without laser irradiation)

5. PDT with low PS concentration (5.0 mg/kg FC$_4$S i.p. to tumor-bearing mice followed by 100 J/cm^2 laser irradiation)

6. PDT with moderate PS concentration (10 mg/kg FC$_4$S i.p. + 100 J/cm^2 laser irradiation) and

7. PDT with high PS concentration (15 mg/kg FC$_4$S i.p. + 100 J/cm^2 laser irradiation).

2.4.4. Laser Irradiation—Before irradiation, the PS-injected mice were kept in a dark room for a period of 24 h to allow bio-distribution of FC$_4$S to the tumor site after intraperitoneal injection of water-soluble FC$_4$S in phosphate-buffered solution (5–15 mg/kg body weight) at a site roughly 2.0 cm away from the tumor location. Prior to light irradiation, the mouse was anesthetized by avertin (0.3 mL/mouse) and the hair on and around the tumor site removed. The tumor site was subsequently irradiated with an argon ion laser beam (Spectra Physics, Model 168) at a wavelength of 514.5 nm. The beam was delivered via a quartz fiber with the circular area of illumination output focused to a diameter of 7–8 mm with the total light dose adjusted to 100 J/cm^2 in each experiment (180 mW/cm^2 for 10 min).

2.4.5. Data Collection—Animals were examined every 5 days after the treatment for a period of 30 days. The responses were evaluated by measuring the animal average body weight and tumor volume (length $\times$ width^2)/2.[11] 30 days following treatment, animals were euthanized using carbon dioxide chamber. The final body weight and organ weights, including liver, kidney, spleen, heart, and tumor, were measured. Blood samples were drawn for relative white blood cell counting and biochemistry. Subpopulations of blood leukocytes were determined by Liu's staining as described. Anti-coagulated blood was air-dried on a slide and covered by solution A (eosin Y) for 40 sec. The slides were immersed in solution B (methylene azure) for 70 sec, washed, and air-dried. The subpopulations of leukocytes,

including monocytes, lymphocytes, and neutrophils were determined by differentially counting 200 leukocytes under a microscope (Nikon ECLIPSE E 200, 1000×).

The plasma biochemistry analyses were performed with a Hitachi 7050 Automatic Analyzer in order to determine the levels of aspartate aminotransferase, alanine aminotransferase, alkaline phosphatase, creatinine, total protein, albumin, blood urea nitrogen, triacylglycerol, and glucose.

2.5. Statistical Methods

All data collected from cells and mice were analyzed by the statistical software, SAS (Version 9.1.3) using General liner model (GLM). Differences between the treatments were analyzed and compared by Duncan's multiple comparison. A p-value of <0.05 was considered significant.

3. RESULTS AND DISCUSSION

3.1. Photoirradiated FC$_4$S Generates Singlet Oxygen and Superoxide Radical Anion

Direct measurement of singlet oxygen was carried out by the detection of luminescence at 1270 nm. The result of the luminescence intensity of singlet oxygen generated from 10 μM of FC$_4$S in DMF, DMSO, H$_2$O, and PBS under 512 nm and 600 nm pulsed laser irradiation is shown in Figures 1(B) and (C). The highest intensity of luminescence was detected in DMF, followed by DMSO $\gg$ H$_2$O. This observation is consistent with the lifetime of singlet oxygen having been reported as 25, 30, 9.8, and 3.2 μsec in the solvents DMF,[22] DMSO,[22] and H$_2$O,[23] respectively. The lifetime is roughly 10 times longer in DMF than in H$_2$O. A similar solvent-dependent intensity ratio was also obtained in Figure 1(C) when photoexcitation was induced with a 600 nm pulsed laser. An overall high quantum yield of energy-transfer to molecular oxygen from the triplet hexafunctionalized fullerene cage even under low level excitation was observed.

When FC$_4$S was irradiated in H$_2$O in the presence of molecular oxygen, superoxide radical anions were generated *in situ*. The extent of cytochrome c reduction was shown by the increase in intensity of the optical absorbance at 550 nm, corresponding to the increase in quantity of the reduced ferrocytochrome c. The reduction process of ferricytochrome c leading to formation of ferrocytochrome c was initiated by one-electron transfer from superoxide radical, produced during the PDT process. Production of superoxide radicals was observed to increase in quantity in a dose-dependent manner with the concentration of FC$_4$S increasing from 0.0, 12.5, 25.0, to 37.5 μM (Fig. 2(A)). The production of superoxide radicals was also detected to increase in quantity in a time-dependent manner with a constant concentration of FC$_4$S at 12.5 μM. A gradual increase in quantity of superoxide radicals was observed upon increasing the irradiation time from 0 to 90 min.

In a separate experiment, the presence of superoxide radical in the solution was confirmed by application of superoxide dismutase (SOD, 75 or 150 units) for selective removal of superoxide that was produced by reaction of the photoexcited FC$_4$S molecules with molecular oxygen. A high $O_2^{-\bullet}$ production rate using a constant concentration of FC$_4$S at 12.5 μM and irradiation for a period of 90 min was suppressed by addition of SOD. The data

established the linear correlation between the optical absorbance at 550 nm and the quantity of $O_2^{-\bullet}$ produced by FC$_4$S.

3.2. Possible Photochemical Mechanisms in Biological Systems

Singlet oxygen formed by the action of light on PS molecules in biological systems is widely regarded as the main cytotoxic agent in PDT action.[24] In addition, after intersystem crossing to the triplet state, the sensitizer also can participate in electron transfer processes, leading to radical formation (Type I reaction).[25] In biological systems, large amounts of reducing agents (such as NADH, FADH$_2$, NADPH etc.) are widely distributed in cytoplasm, and in organelles such as mitochondria. The possibility has been raised that singlet oxygen could oxidize mitochondrial components via one-electron redox reactions with concomitant formation of superoxide radicals ($O_2^{-\bullet}$). Since the cumulative energy released at each step along the electron-transport chain is utilized in the conversion of ADP into ATP, maximum interference with the metabolic process would arise if singlet oxygen oxidized the first component of the chain, NADH.[26] In such a scheme, not only would mitochondrial energy production be prevented, but also the potential cytotoxic superoxide radical would be generated at a locus where the cell may be more susceptible to oxidative damage.

We investigated whether either the triplet state of FC$_4$S or singlet oxygen could react with (or be quenched by) an electron donor, NADH, which was added to a cuvette to effect the electron-transfer process in the photoirradiated FC$_4$S system. As shown in Figure 2(B), the decay of 1270 nm luminescence was observed to be dependent on the concentration of NADH. This decay curve can be roughly separated into 3 regions, first, without addition of NADH and a molar ratio of FC$_4$S to NADH of around 1 to 10. Second, a molar ratio of FC$_4$S to NADH is around 1 to 50–125. And third, the molar ratio is more than 1 to 250. In the first group, singlet oxygen decay was quenched by solvent. The second group shows, when the molar ratio reached around 1 to 100–125, the decay of singlet oxygen increased but the maximum luminescence still reminded the same. In the third group, singlet oxygen decay rate increased, and the maximum luminescence decreased.

The time-resolved luminescence of singlet oxygen, or the monoexponential decay of singlet oxygen in solution can be simplified and expressed by Eq. (1). By fitting a kinetic curve of the phosphorescence signal to Eq. (1) (18), then analyzing the data using commercial software (nmnlfit.m, Metlab 5, Mathworks Inc., Natick, MA), with τ_T (triplet state photosensitizer lifetime), τ_D (singlet oxygen lifetime), and A ($= N\sigma[S_0]\,\Phi_D$ as free parameters as described previously.[19] Lifetime of triplet state PS and singlet oxygen can be determined by fitting the kinetic model.

$$[^1O_2](t) = N\sigma[S_0]\Phi_D(\tau_D/\tau_T - \tau_D) \times [exp(-t/\tau_T) - exp(-t/\tau_D)] \quad (1)$$

$$FC_4S \xrightarrow{h\nu} {}^1FC_4S^* \xrightarrow{isc} {}^3FC_4S^* \xrightarrow{k_1} {}^1O_2 \xrightarrow{k_d} {}^3O_2 \quad (2)$$

$$^1O_2 + NADH \xrightarrow{k_q} NAD^{\bullet} + O_2^{-\bullet} + H^+ \quad (3)$$

For the first order reaction, $^1O_2 \rightarrow {}^3O_2$ (Eq. (2)), the reciprocal of the measured singlet oxygen lifetime (τ_D, supplementary Table S1) represents the decay rate (k_{obs}, Table S1) of singlet oxygen. After light irradiation, triplet state FC$_4$S transfers energy to oxygen leading to singlet oxygen formation. Before adding NADH, singlet oxygen luminescence is determined by the rate constant k_1, which represents the singlet oxygen generated from triplet state FC$_4$S, and k_d, the quenching effect of solvent (D$_2$O:H$_2$O = 3:1). Lifetime of singlet oxygen in D$_2$O/H$_2$O mixture was 13 μs, corresponding to the decay rate 7.5×10^4 s^{-1}. After adding NADH, accelerates the decay of singlet oxygen, i.e., singlet oxygen is quenched by NADH. The maximum luminescence of singlet oxygen (Table S1, column 3) generated from FC$_4$S is controlled by k_1. The sum of luminescence signals over the first 50 μs represents the generation and deactivation of singlet oxygen. This integrated area is controlled by rate constant k_1, k_d, and k_q (whenever a singlet oxygen quencher is put into the homogeneous system). Without NADH, a strong signal was detected as shown in Figure 2(B) (1:0). It shows that the rate constant k_1 is much greater than k_d. When 10 times NADH added to this system, maximum luminescence remind the same, but the integrated area decreased, means that k_1 is greater than 10 times k_q plus k_d. At this time, the singlet oxygen was quenched by NADH and lead to the generation of superoxide radicals ($O_2^{-\bullet}$, Eq. (3)). Same as molar ratio of FC$_4$S to NADH equals to 1 to 100. When the concentration of NADH reached to 250 times than FC$_4$S maximum luminescence decreased, so the rate constant k_1 is less than 250 times k_q plus k_d. Another possibility is NADH reacts with triplet state FC$_4$S.

The triplet state lifetime (τ_T) values of FC$_4$S measured with different FC$_4$S/NADH ratios were also summarized in Table S1 (supporting information). From molar ratio 1 to 0 to 1 to 1000, the decay of triplet state FC$_4$S was accelerated when the FC$_4$S/NADH ratio reached to 1 to 1000 showing that triplet state FC$_4$S also has the ability to react with NADH. According to the chemical properties of fullerene derivatives they are electrophilic able to accept several electrons. In this homogenous system, the main factor deciding which molecule (triplet state FC$_4$S or singlet oxygen) will react with NADH first, relies on which reduction potential is closer to NADH.

The Stern-Volmer relationship.[27] describes the increase in the pseudo-first order decay rate constant upon addition of a quencher in a homogeneous system. By plotting the reciprocal of the measured singlet oxygen lifetime versus NADH concentration, the observed data can be well fitted to a linear regression curve ($R^2 = 0\ 9898$) (Fig. 2(C)). Its slope shows the quenching rate=constant of k_q which was calculated as 3.5×10^7 M^{-1}s^{-1}. This is consistent with the quenching constant of $8{-}10 \times 10^7$ M^{-1}s^{-1} from reported data.[28] The rate constant k_1 can be estimated as $3{-}8 \times 10^9$ s^{-1}, which represents the efficiency of triplet state FC$_4$S in generating singlet oxygen.

3.3. *In Vitro* Cytotoxicity by Photoactivated FC$_4$S

The changes in cell morphology after PDT are shown in Figures 3(a)–(d). Without addition of FC$_4$S, 40 min light exposure did not damage the cells nor alter the cell morphology. After PDT (40 min light; 8 mW/cm^2, 20 J/cm^2, 5.0 μM FC$_4$S) all tumor cells were damaged and fragmented. Cells were condensed, shrunken, with some vacuoles seen in the cytoplasm. A largely deteriorated cellular appearance with a damaged cell membrane was observed. The results indicated an good PDT effect of FC$_4$S in destroying fibrosarcoma cells.

The quantitative cellular cytotoxicity results are summarized in Figures 3(e) and (f), showing a decrease of cell viability in both cell lines (HT1080 in Fig. 3(e) and S180 in Fig. 3(f)) that was both dose-dependent and irradiation time-dependent. Viability was reduced to the limit of detection (<5% survival) by the combination 5.0 μM of FC$_4$S and 30 min light. In the absence of light, proliferation of the tumor cell was inhibited only at high concentrations of FC$_4$S (>10 μM). While PDT killing was broadly similar for both cell lines, it appeared that S180 cells were somewhat more susceptible that HT1080 cells.

3.4. S180 Tumor Growth and Mouse Body and Organ Weights

After mice with tumors were followed for one month, the mice in Groups 2 (untreated tumor), 3 (light control), and 4 (dark control) had been sacrificed due to excessive size of the tumor (usually around day 26); however those in Groups 1 (no tumor), 5, 6, and 7 (PDT groups) (Table I) survived and in groups 5–7 the tumors were well controlled. These results were in agreement with the results by Hau et al.,[29] who found that during the 120-d experimental period, the tumor tissue grew fastest within the first 60 d. When the tumor weight was subtracted from the weight of the mice when the mice were sacrificed at day 30, the average weights of Groups 2, 3, and 4 were less than those of the other treatment groups. The mean body weight after subtracting the tumor for Groups 2, 3, and 4 were 84%, 87%, and 88% of the original weights, respectively. Therefore, 12–16% of the total body weight of these 3 groups was caused by the rapid tumor growth.

In this study, the relative organ weights of mice that were sacrificed at 30 d were compared and the results showed that the spleens of mice with tumors was affected the most (2.7 times that of the no tumor control, Group 1). Furthermore, after receiving PDT, no reductions in splenomegaly were observed even though the tumor weights were significantly reduced. A previous study showed that the DNA synthesis rate in spleen cells declined within 3 d of tumor cell inoculation and subsequently gradually recovered; up to day 33, when the DNA synthesis rate in the spleen was higher than that for the control group.[30] The spleen is a lymphoid organ containing lymphocytes (LYMs) and monocytes (MONs) in normal animals. It is thought that the splenomegaly frequently observed in tumor bearing mice is due to rapid proliferation of suppressor cells in lymphoid organs such as the spleen. These suppressor cells are required to permit tumor growth in immune-competent mice. These suppressor cells may be CD11b + Gr-1+ myeloid derived suppressor cells[31] and/or CD4$^+$CD25$^+$foxp3$^+$ regulatory T-cells.

The mean kidney weights of Group 7 were significantly higher than those of Group 2 ($p < 0$ 05). Group 4–7 exhibited high kidney weights, possibly because of the effect of FC$_4$S, since

high doses of FC_4S have been reported to be toxic to kidney.[13] The liver weight of Group 4 was significantly higher than that of Group 1 and the liver of Groups 3–7 were higher than those of Groups 1 and 2. The tumor weights of the untreated and control Groups 2–4 were 16%, 11.5%, and 12% of their body weight, respectively. The 100 J/cm² of laser irradiation (Group 3) and injections of 15 mg/kg FC_4S (Group 4) slightly inhibited tumor growth but not significantly. There were highly significant differences between the tumor weights of Groups 2–4 and the PDT Groups 5–7 ($p < 0.001$). Among Groups 5–7 the tumor weight decreased when the FC_4S dose increased.

3.5. Inhibitory Effects of FC_4S, Laser and PDT on Tumor Growth

Figures 4(A) and (B) show representative images of a mouse with an untreated tumor (Fig. 4(A)) and a tumor treated with high dose PDT (Fig. 4(B)). Figure 4(C) shows the mean tumor size growth curves between day 0 and day 30. The tumor growth in Groups 2–4 (tumor control, light alone, and FC_4S dark), increased from 320 mm³ to 5000 mm² (maximal permitted volume), which usually occurred about day 26. On day 30, the tumor sizes of the PDT Groups 5, 6, and 7 were only 7, 6, and 5 times the original tumor sizes, respectively. If the tumor volume of Group 2 was considered as 100%, then the tumor sizes of Groups 3–7 were 62%, 75%, 20%, 17%, and 17%, respectively. Therefore, combining 5–15 mg/kg FC_4S with 100 J/cm² of laser light therapy inhibited tumor growth by >80%.

PDT-treated tumor-bearing mice exhibited 3 possible outcomes.

1. A complete recovery: The tumors disappeared completely after 30 d or only scars remained (Fig. 4(B)).

2. Partial recovery: Tumor tissue remained after 30 d, but the tumor volume was less than 1000 mm³ and the tumor tissue grew slowly. In 2 mice that received 10 mg/kg of FC_4S and 100 J/cm² of laser irradiation, the tumor volume first decreased and later increased.

3. No effect: Tumor tissue continued to grow rapidly after PDT therapy. Table S2 shows the distribution of these 3 outcomes in the various treatment groups.

The tumor size of the PDT treatment group that received 15 mg/kg FC_4S decreased the fastest. On the third day after laser irradiation, 2 mice exhibited smaller tumor sizes than before the treatment, which explains the reason that the tumor volume of Group 7 was smaller than that of Groups 5 and 6 within 0–15 d. The inhibitory effects on tumor growth in Groups 5 and 6 can only be seen 15 days after irradiation. The objective of this experiment was to investigate whether *in vivo* treatment using FC_4S photosensitizer could destroy the tumors. Therefore, in this experiment, the mice received a 1-time FC_4S intraperitoneal injection and a 1-time laser light irradiation only.

3.6. Effects of FC_4S, Laser and PDT on Improvement in Hematology and Blood Biochemistry

The values of lymphocytes (LYM), monocytes and neutrophils as a % of total leukocytes are shown in Table II. There were no statistically significant differences in monocytes so the

following discussion concentrates on LYM and neutrophils. On day 30 after the mice were inoculated with S180 cells, the percentages of blood LYM and neutrophils were substantially different from those of the control group. The ratio of LYM to neutrophils was 3:1 (69% vs. 23%) in Group 1 (healthy mice) and was 1:1 (51% vs. 42%) in the tumor-bearing group (Group 2). Hau et al.[30] reported that tumor growth increased the total leukocyte level to 4 times that of the control group (28.4 $10^3/mm^3$ vs. 7.0 $10^3/mm^3$ and the percentage of LYM and neutrophils became 45% and 41% with tumor growth versus 83% and 14% in the control group. Therefore, tumor growth caused overall leukocyte proliferation while relatively decreased lymphocytes and increased neutrophil levels.

As shown in Table II, the percentage of neutrophils in laser alone treated Group 3 was significantly higher than that for Groups 1 and 4–7 ($p < 0.05$) and LYM were lower. In other words the laser alone tended to even further increase the changes caused by tumor growth. The dark PS alone Group 4 showed a non-significant improvement manifested by an increase in LYM and a reduction in neutrophils compared to tumor bearing mice. The high dose PDT Groups 6 and 7 showed significant increases in LYM versus laser alone treated tumor mice (Group 3) and also significant reductions in neutrophils versus Group 3.

We studied the effects of tumor growth on blood biochemistry, and the effects of fullerene-PDT on improving blood biochemistry. As shown in Table III, the AST and LDH levels in the tumor-bearing group (Group 2) were significantly higher than those in naive Group 1 while Alb levels were lower. These findings are in agreement with the fact that there are higher AST and LDH levels in patients with tumors compared with those of healthy people, and the albumin (Alb) levels in patients with tumors are lower compared with those of healthy people.[32] The alkaline phosphatase (ALP), creatinine (Crea), cholesterol (Chol), and Glucose (Glc) levels in the tumor-bearing group were significantly lower compared with those in Group 1 ($p < 0.05$). This is in broad agreement with the variations in metabolism seen in patients with cancer.[33] The groups that received laser irradiation alone, FC_4S intraperitoneal injection, or PDT showed lower AST activity. The numerical values for Groups 3, 5, and 7 were significantly lower than those for Group 2 ($p < 0.05$). Finally, the ALP, Crea, Chol, and Glc numerical values in the PDT-treated group were brought nearer to those in healthy mice (Group 1).

The LDH numerical values for Groups 3–7 were higher than those of Group 2. It was shown that RBCs treated with PDT damaged the cells and caused hemolysis[34] and release of LDH, which could explain the reason that in this study, LDH levels in Groups 3, 5, 6, and 7 were high. The LDH levels in blood cells are 10 times the levels in tissue. Potentially, during blood sampling, if the fragility of RBCs in Groups 3, 5, 6, and 7 increased, LDH could be released, thereby causing high LDH values, despite that hemolysis could not be observed with the naked eye. Another reason could be that PDT causes pathological changes in other tissue, which has not been detected. The reason for high LDH levels in Group 4 is currently unknown.

3.7. Mechanisms of Therapeutic Effects

PDT can destroy tumor cells because of the generation of reactive oxygen species (ROS) produced from $^1O_2$ by energy conversion and $O_2^{-\bullet}$ by electron transfer causing oxidative

damage.[2] ROS can oxidize Chol, phospholipids, and proteins in cells[35][36] and the cell membrane lipids are susceptible to free radical attacks, thereby causing lipid peroxidation. In addition, $^1O_2$ damages the structures of certain amino acids (e.g., His, Lys, Met, Tyr, and Trp), causing cross-linking.[37][38] Once the structure of a cell membrane is damaged, the permeability of the cell membrane changes.

The curative effect of PDT may be partially because of tumor vascular necrosis caused by the oxidative damage to tumor endothelial cells.[39] However in the present study the FC_4S was injected i.p. rather than i.v. This is expected to mean that relatively smaller amounts of FC_4S would be present in the tumor blood vessels at the time of laser irradiation, than would be expected if the FC_4S had been injected i.v.

The expression level of tyrosine kinase in normal cells is typically low, whereas high tyrosine kinase activity is found in tumor cells.[40] Therefore, growth factors, such as epidermal growth factor, can stimulate the formation of vascular endothelial growth factor through the function of protein kinase c (PKC). It is known[41] that inhibitors of tyrosine kinase or PKC also suppress the formation of tumor blood vessels. Lu et al.[42] studied the inhibition of tyrosine kinase and PKC activities mediated by application of the C60 fullerene derivative F1 without light exposure. This study may explain why tumor growth in the 15-mg/kg FC_4S-treated dark control Group 4 was inhibited and why hematological and blood biochemistry was also improved in this group that received no light. The reason why laser alone had an inhibitory effect on tumor growth may be due to a laser-induced hyperthermia effect on the tumor. Previous studies with interstitial laser irradiation of tumors have shown a therapeutic effect.[43]

4. CONCLUSION

Functionalization of C_{60} by attachment of 6 *n*-butyl sulfonic acid salt to the structure of FC_4S in a form of self-assembled molecular micellar nanospheres was found to retain high efficiency in generating singlet oxygen upon irradiation with a visible light. The production of $^1O_2$ was confirmed by direct detection of its near-infrared luminescence at 1270 nm. The quantum yield of FC_4S for the generation of $^1O_2$ in H_2O was roughly estimated to be 0.36 using the relative correlation to that of C_{60}/γ-CD.[44] The mechanism was correlated to the facile intermolecular triplet energy-transfer from photoexcited $^3FC_4S^*$ to molecular oxygen. We also demonstrated that, in the presence of electron donor, such as cytochrome *c* or NADH, photoinduced intramolecular electron-transfer from NADH to either excited singlet $^1FC_4S^*$ or triplet $^3FC_4S^*$ acceptor states can occur in a dose-dependent manner, following by the subsequent electron-transfer from the resulting fullerenyl anion radical, (FC S)$^{-\bullet}$, to O_2 forming superoxide radical ($O_2^{-\bullet}$).

Both $^1O_2$ and $O_2^{-\bullet}$ (subsequent conversion to $HO^\bullet$) are widely believed to post the major cytotoxic effect to diseased cells in photodynamic therapy. Based on the *in vitro* and *in vivo* results, photoactivated FC_4S molecular micelles were found to kill tumor cells and inhibit tumor growth effectively. High water-solubility of FC_4S with large molecular charge polarity (6 sulfonate anions per molecule) allows it to be injected i.p. and circulate to the tumor, where it can be efficiently photoactivated by an argon laser.

This study has shown that the improvement in leukocyte levels and blood biochemistry of PDT-treated groups is probably a result of tumor growth inhibition, which improves the physiology of the mice to more nearly resemble that of healthy mice. However it is also possible that PDT directly affects the hematopoietic systems by cytokines released during PDT.

Supplementary Material

Refer to Web version on PubMed Central for supplementary material.

Acknowledgments

References and Notes

1. Kharkwal GB, Sharma SK, Huang YY, Dai T, Hamblin MR. Lasers Surg Med. 2011; 43:755. [PubMed: 22057503]

2. Agostinis P, Berg K, Cengel KA, Foster TH, Girotti AW, Gollnick SO, Hahn SM, Hamblin MR, Juzeniene A, Kessel D, Korbelik M, Moan J, Mroz P, Nowis D, Piette J, Wilson BC, Golab J. CA Cancer J Clin. 2011; 61:250. [PubMed: 21617154]

3. Wilson BC, Patterson MS. Phys Med Biol. 2008; 53:R61. [PubMed: 18401068]

4. Arbogast WJ, Darmanyan PA, Foote SC, Diederich NF, Whetten LR, Rubin Y, Alvarez MM, Anz JS. J Phys Chem. 1991; 95:11.

5. Yamakoshi Y, Umezawa N, Ryu A, Arakane K, Miyata N, Goda Y, Masumizu T, Nagano T. J Am Chem Soc. 2003; 125:12803. [PubMed: 14558828]

6. Li Y, Huang Y, Du S, Liu R. Chem Phys Lett. 2001; 335:524.

7. Hu Z, Zhang C, Huang Y, Sun S, Guan W, Yao Y. Chem Biol Interact. 2012; 195:86. [PubMed: 22108244]

8. Tegos GP, Demidova TN, Arcila-Lopez D, Lee H, Wharton T, Gali H, Hamblin MR. Chem Biol. 2005; 12:1127. [PubMed: 16242655]

9. Lu Z, Dai T, Huang L, Kurup DB, Tegos GP, Jahnke A, Wharton T, Hamblin MR. Nanomedicine (Lond). 2010; 5:1525. [PubMed: 21143031]

10. Sharma SK, Chiang LY, Hamblin MR. Nanomedicine (Lond). 2011; 6:1813. [PubMed: 22122587]

11. Tabata Y, Murakami Y, Ikada Y. Jpn J Cancer Res. 1997; 88:1108. [PubMed: 9439687]

12. Mroz P, Xia Y, Asanuma D, Konopko A, Zhiyentayev T, Huang YY, Sharma SK, Dai T, Khan UJ, Wharton T, Hamblin MR. Nanomedicine. 2011; 7:965. [PubMed: 21645643]

13. Chen HHC, Yu C, Ueng TH, Liang CT, Chen BJ, Hong CC, Chiang LY. Fullerene Sci Techn. 1997; 5:1387.

14. Chen HH, Yu C, Ueng TH, Chen S, Chen BJ, Huang KJ, Chiang LY. Toxicol Pathol. 1998; 26:143. [PubMed: 9502397]

15. Yu C, Canteenwala T, El-Khouly ME, Araki Y, Pritzker K, Ito O, Wilson BC, Chiang LY. J Mater Chem. 2005; 15:1857.

16. Yu C, Canteenwala T, Chiang LY, Wilson B, Pritzker K. Synthetic Met. 2005; 153:37.

17. Yu C, Bhonsle JB, Huang JP, Shiea J, Chen BJ, Chiang LY. Chem Lett. 1998; 27:465.

18. Jeng US, Lin TL, Tsao CS, Lee CH, Canteenwala T, Wang LY, Chiang LY, Han CC. J Phys Chem B. 1999; 103:1059.

19. Niedre M, Patterson MS, Wilson BC. Photochem Photobiol. 2002; 75:382. [PubMed: 12003128]

20. Mosmann T. J Immunol Methods. 1983; 65:55. [PubMed: 6606682]

21. Gurley AM, Hidvegi DF, Bacus JW, Bacus SS. Cytometry. 1990; 11:468. [PubMed: 1693113]

22. Darmanyan PA. Khim Fiz. 1987; 6:1192.

23. Patterson MS, Madsen SJ, Wilson BC. J Photochem Photobiol B. 1990; 15:69. [PubMed: 2111394]

24. Schmidt R. Photochem Photobiol. 2006; 82:1161. [PubMed: 16683906]

25. Kruft BI, Greer A. Photochem Photobiol. 2011; 87:1204. [PubMed: 21883245]

26. Halliwell, B.; Gutteridge, JMC., editors. Free Radicals in Biology and Medicine. 2nd. Clarendon Press; Oxford: 1989.

27. Hall RD, Chignell CF. Photochem Photobiol. 1987; 45:459. [PubMed: 3575442]

28. Buettner GR, Hall RD. Biochim Biophys Acta. 1987; 923:501. [PubMed: 3030441]

29. Hau DM, Chang H, Hsu HY. Taiwan Yi Xue Hui Za Zhi. 1987; 86:615. [PubMed: 3655706]

30. Hau DM, Wang Ll, Chang HY. Acupuncture Res Quarterly. 1986; 1:1.

31. Watanabe S, Deguchi K, Zheng R, Tamai H, Wang LX, Cohen PA, Shu S. J Immunol. 2008; 181:3291. [PubMed: 18714001]

32. Gupta D, Lis CG. Nutr J. 2010; 9:69. [PubMed: 21176210]

33. Zhang Y, Yang JM. Cancer Biol Ther. 2013; 14:81. [PubMed: 23192270]

34. Malik Z, Djaldetti M. Int J Cancer. 1980; 26:495. [PubMed: 6941938]

35. Kessel D. Biochemistry. 1977; 16:3443. [PubMed: 196633]

36. Girotti AW, Lyman S, Deziel MR. Photochem Photobiol. 1979; 29:1119. [PubMed: 504349]

37. Goldstein BD, Harber LC. J Clin Invest. 1972; 51:892. [PubMed: 5014616]

38. Schothorst AA, van Steveninck J, Went LN, Suurmond D. Clin Chim Acta. 1972; 39:161. [PubMed: 5038747]

39. Abels C. Photochem Photobiol Sci. 2004; 3:765. [PubMed: 15295633]

40. Wang ZY, Zhang Q, Wilson J, Ratajczak MZ, Wasik MA. J Mol Diagn. 2003; 5:113. [PubMed: 12707376]

41. Perona R. Clin Transl Oncol. 2006; 8:77. [PubMed: 16632420]

42. Lu LH, Lee YT, Chen HW, Chiang LY, Huang HC. Br J Pharmacol. 1998; 123:1097. [PubMed: 9559892]

43. Muralidharan V, Malcontenti-Wilson C, Christophi C. J Gastrointest Surg. 2001; 5:646. [PubMed: 12086904]

44. Yu C, Canteenwala T, El-Khouly ME, Araki Y, Pritzker K, Ito O, Wilson BC, Chiang LY. J Mater Chem. 2005; 15:1857.

Highlights

- A hexa-sulfonated C60 fullerene (FC$_4$S) has been tested for photodynamic therapy (PDT) of cancer *in vivo*.

- Photoexcited FC$_4$S produced both singlet oxygen and superoxide and carried out PDT kililng of cancer cells.

- After IV injection into tumor-bearing mice argon laser irradiation of tumors produced 80% reduction in tumor volume compared to controls.

- Hematological and blood biochemistry parameters were improved by PDT.

- This study may have clinical application in nanomedicine.
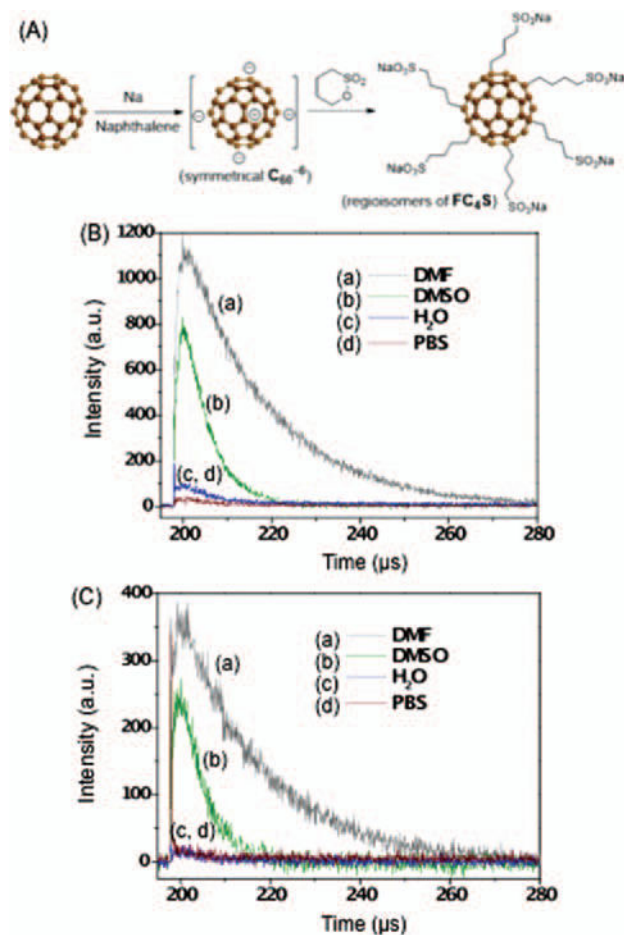
Figure 1.
(A) Synthetic scheme and the chemical structure of molecular micellar hexa(sulfo-*n*-butyl)fullerene (FC$_4$S) in a form of sodium salt. Time-resolved $^1O_2$ luminescence produced upon laser irradiation of FC$_4$S at (B) 512 nm and (C) 600 nm excitation in different solvents: (a) DMF, (b) DMSO, (c) H$_2$O, and (d) phosphate buffer solution (PBS).
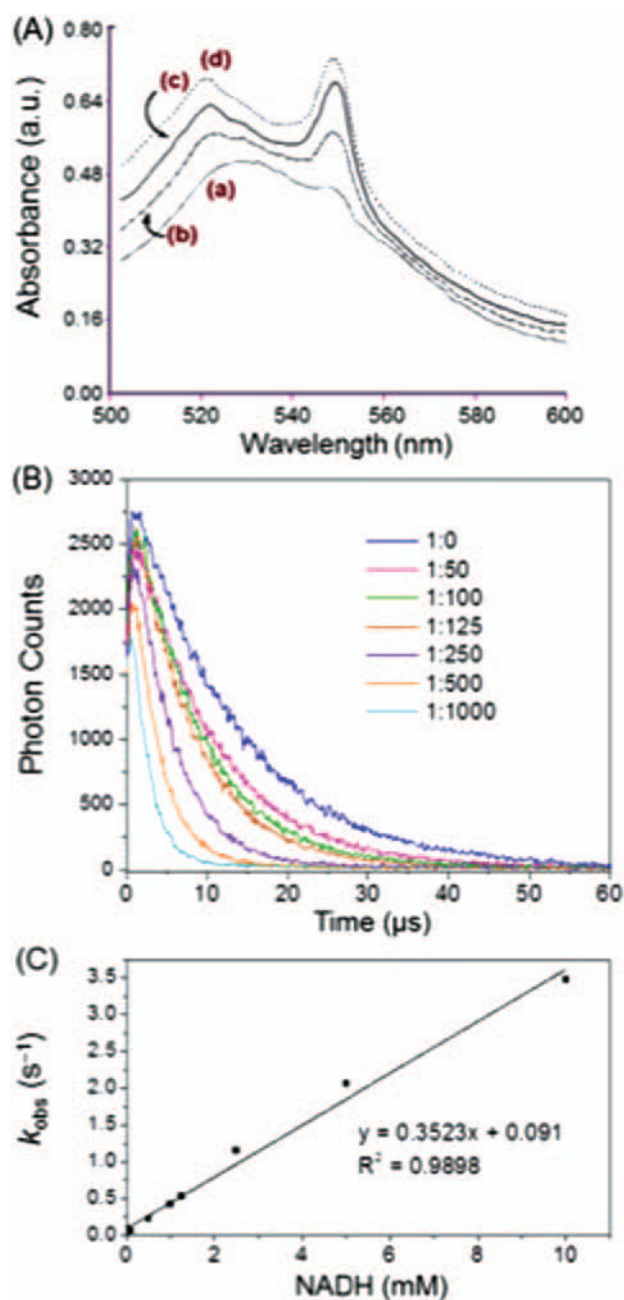
Figure 2.
(A) Dose-dependent superoxide radical production by FC$_4$S at concentrations: (a) none, (b) 12.5 μM, (c) 25.0 μM, and (d) 37.5 μM under fluorescence light excitation (27 W) in the presence of cytochrome c. (B) Time-resolved ^{1}O$_2$ luminescence emission from FC$_4$S (10 μM) in D$_2$O–H$_2$O (3:1) in the presence of an increasing concentration of NADH (molar ratio of FC$_4$S:NADH from 1:0 to 1:1000), under photoexcitation using a crystal pulse laser at 532 nm. (C) Plot of k_{obs} (1/lifetime of singlet oxygen, s^{-1} versus NADH concentration.
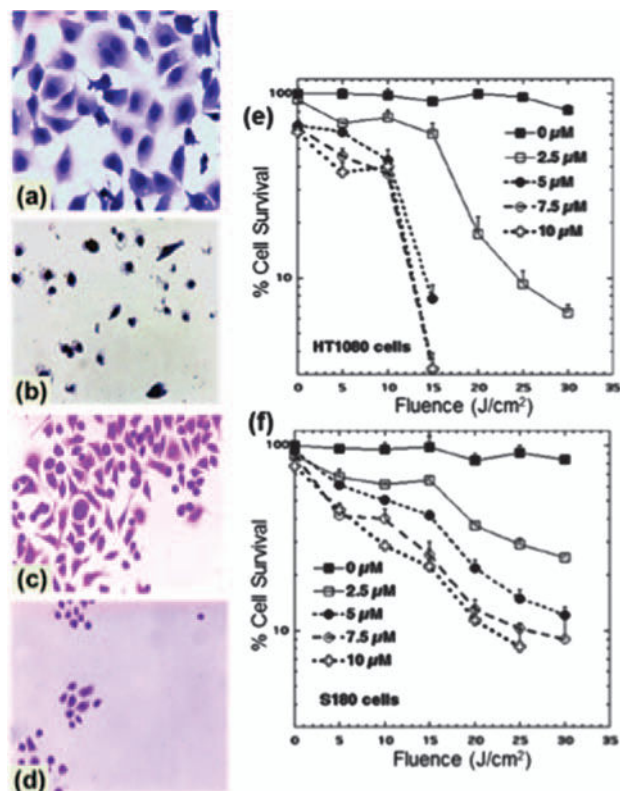
Figure 3.
Cell morphological changes with (b, d) and without (a, c) the addition of FC_4S (5 μM) followed by broad-band light irradiation (8 mW/cm^2 for a period of 40 min. (a), (b) are human fibrosarcoma cells and (c), (d) are murine sarcoma 180 cells. (a), (b) Giemsa stain $\times$ 400; (c), (d) Feulgen stain $\times$ 400. Killing of human fibrosarcoma cells (e) and murine sarcoma 180 cells (f) by PDT, with the addition of FC_4S (0–10.0 μM) and fluorescence light irradiation for 0–60 min (0–30 J/cm^2. Each data point represents mean $\pm$ SE of 4 replicates.
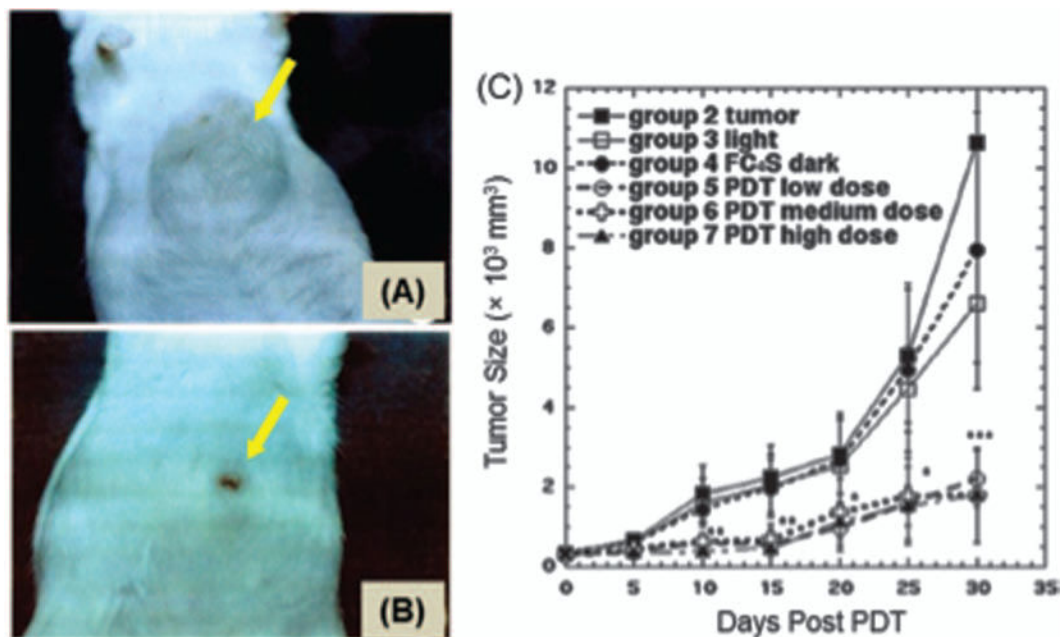
Figure 4.
Representative pictures of ICR mice with S180 tumors growing for 30 days after being (A) untreated; (B) treated with intraperitoneal injection of FC_4S (5.0 mg/kg) combined with laser (100 J/cm^2 irradiation. (C) Tumor size growth curves of: tumor untreated control, 100 J/cm^2 laser alone, 15 mg/kg FC_4S (i.p.) dark control, 5.0 mg/kg FC_4S (i.p.) + 100 J/cm^2 laser, 10 mg/kg FC_4S (i.p.) 100 J/cm^2 laser, and 15 mg/kg FC_4S (i.p.) + 100 J/cm^2 laser irradiation. Each data represents mean SE ± of 10 mice. $*p < 0\ 05$; $**p < 0\ 01$; $***p <+0\ 001$ PDT groups versus control groups.

Table I

Body, tumor weights and organ weight ratio of mice in the control and tumor-bearing groups receiving 100 J/cm^2 laser irradiation, FC$_4$S injected (i.p.), and the combination (PDT in three doses).

Group[1]	Body weight (g)		Organ weight ratio (%)[4]			
	Day 30[2]	B.W.-T.W.[3]	Liver	Kidneys	Spleen	Tumor
1	41.69 ±0.725		5.58±0.14^b	1.87 ± 0.06^{a,b}	0.37 ±0.02^b	0.00^d
2	44.17 ±1.06	39.17±1.28	5.99 ±0.41^{a,b}	1.74±0.10^b	1.01 ±0.10^a	11.24±3.36^a
3	44.85 ±2.15	39.83 ±2.24	6.70 ± 0.50^{a,b}	1.94 ± 0.08^{a,b}	1.07 ±0.18^a	11.45 ± 2.48^{a,b}
4	43.25 ±0.76	39.17 ±1.69	6.81±0.21^a	2.01 ± 0.06^{a,b}	1.15 ±0.10^a	11.50 ± 2.20^{a,b}
5	41.41 ±0.7	39.97 ±0.9	6.77 ± 0.25^{a,b}	2.00 ± 0.04^{a,b}	1.13 ±0.11^a	3.48±1.06^{c,d}
6	41.69 ±2.24	40.83 ±2.37	6.53 ± 0.40^{a,b}	1.93 ± 0.09^{a,b}	0.97 ±0.14^a	2.00 ± 1.20^{c,d}
7	40.58 ±0.85	39.80 ±1.02	6.43 ± 0.40^{a,b}	2.16±0.18^a	0.98 ±0.16^a	1.93 ± 1.62^{c,d}

Notes:

[1] See materials and methods for detail;

[2] Mice were sacrificed 30 days after FC$_4$S injection or earlier if tumors exceeded a certain size;

[3] The body weight of mice minus the tumor weight in grams at day 30;

[4] Organ or tumor weight as a % of body weight;

[5] Values are mean ±SE of 10 mice.

[a, b, c, d] Values in the same column without the same superscripts are significantly different ($p < 0.05$).

Table II

Comparison of the percentages of lymphocytes, monocytes, and neutrophils of mice in the control and in tumor-bearing groups receiving 100 J/cm^2 laser irradiation, FC$_4$S injected (i.p.), and the combination (PDT in three doses).

Group[1]	Lymphocyte (%)	Monocyte (%)	Neutrophil (%)
1	69.51 ±2.35[2,a]	6.80 ±0.87	23.69 ±2.13[c]
2	50.84 ±4.98[b,c]	6.76 ±1.18	41.90±4.80[a,b]
3	44.46 ±12.15[c]	5.79 ±0.83	49.75±11.51[a]
4	59.25 ± 5.34[a,b,c]	8.47 ±1.00	32.26 ± 5.05[b,c]
5	60.29 ± 3.68[a,b,c]	8.84 ±1.57	30.86±2.61[b,c]
6	61.05 ± 5.55[a,b]	7.07 ±1.10	31.96±5.46[b,c]
7	62.96 ± 3.55[a,b]	10.40 ±2.04	26.63 ± 3.68[b,c]

Notes:

[1] See materials and methods for detail;

[2] Values are mean SE of 10 mice;

[a, b, c] Values in the same column without the same superscripts±are significantly different ($p < 0 05$).

Table III

Blood biochemistry of mice in the control and tumor-bearing groups receiving 100 J/cm² laser irradiation, FC$_4$S injected (i.p.), and the combination (PDT in three doses).

Item	Unit	Group[1]						
		1	2	3	4	5	6	7
AST[2]	(U/L)	163.58 ±34.24^{a,b}	450.91±86.20^a	266.75±35.68^b	330.62 ± 48.66^{a,b}	263.82 ±33.40^b	279.80±51.66^{a,b}	224.63 ±30.02^b
ALT	(U/L)	110.00 ±40.98	81.27 ±11.98	64.00 ±15.82	80.75 ±17.91	91.81 ±15.64	93.90 ±16.61	97.62 ±17.77
ALP	(U/L)	77.00 ±8.02^a	45.82 ±5.28^c	53.00 ±8.75^{b,c}	58.88±5.75^{a,b,c}	69.82 ± 7.47^{a,b}	60.30 ± 5.60^{a,b,c}	63.38 ± 3.20^{a,b,c}
BUN	(mg/dL)	24.18 ± 1.28^{a,b}	23.63 ± 1.46^{a,b}	26.55±4.13^a	24.81 ±1.82^{a,b}	25.54 ±1.16^{a,b}	22.03 ±1.20^{a,b}	20.89 ±1.11^b
Crea	(mg/dL)	0.51 ±0.02^a	0.36 ±0.02^c	0.48±0.03^a	0.46 ± 0.04^{a,b}	0.45 ± 0.02^{a,b}	0.38 ±0.03^{b,c}	0.49 ±0.04^a
TP	(g/dL)	4.43 ±0.17	4.25 ±0.28	4.45 ±0.12	4.43 ±0.18	4.20 ±0.17	4.24 ±0.14	4.68 ±0.17
Alb	(g/dL)	2.30±0.09^a	1.99 ±0.12^{a,b}	1.83±0.20^b	1.93 ±0.09^b	1.92 ±0.08^b	2.13 ± 0.09^{a,b}	2.16 ±0.10^{a,b}
TG	(mg/dL)	49.25 ±9.30	36.91 ±5.09	45.00 ±14.34	41.75 ±6.25	43.18±4.80	35.50 ±5.28	36.00 ±3.65
Chol	(mg/dL)	93.33 ±5.68^a	65.64 ±4.12^{b,c}	57.75 ±7.25^c	68.75 ± 4.21^{b,c}	72.55 ± 4.68^{b,c}	78.90 ± 5.46^{a,b}	81.75±5.83^{a,b}
Glc	(mg/dL)	159.92±9.15^a	103.81±11.01^b	119.75±17.47^{a,b}	130.88 ± 16.02^{a,b}	134.45±6.20^{a,b}	131.90 ± 9.96^{a,b}	140.63 ± 21.71^{a,b}
LDH	(U/L)	1062.00 ±159.31^c	2867.78±737.50^b	4715.75 ±827.30^a	5014.88 ±525.10^a	4682.36±387.27^a	3808.80 ± 278.08^{a,b}	3750.50 ± 397.72^{a,b}

Notes:

[1] See materials and methods for detail;

[2] AST asparate aminotransferase; ALT = alanine aminotransferase; ALP = alkaline phosphatase; BUN = blood urea nitrogen; Crea = creatinine; TP = total protein; Alb = albumin; TG = triglyceride; Chol cholesterol; Glc glucose; LDH lactate dehydrogenase;

[3] Values=are mean SE of 10 mice;

[a,b,c] Values in the same row without the same superscripts are significantly= different ($p < 0.05$).